ACS Chemical Neuroscience

Article

In vivo use of a multi-DNA aptamer-based payload/targeting system to study dopamine dysregulation in the central nervous system

Erin M. McConnell, Katelyn Ventura, Zack Dwyer, Vernon Hunt, Anna Koudrina, Matthew R Holahan, and Maria C. DeRosa

ACS Chem. Neurosci., **Just Accepted Manuscript** • DOI: 10.1021/acschemneuro.8b00292 • Publication Date (Web): 30 Aug 2018

ACS Publications

is published by the American Chemical Society. 1155 Sixteenth Street N.W., Washington, DC 20036

In vivo use of a multi-DNA aptamer-based payload/targeting system to study dopamine dysregulation in the central nervous system

Short title: Use of DNA aptamers in the central nervous system

Erin M. McConnell[1‡], Katelyn Ventura[2‡], Zach Dwyer[2], Vernon Hunt[1], Anna Koudrina[1], Matthew R. Holahan[2] and Maria C. DeRosa[1]

1. **Department of Chemistry, Carleton University, Ottawa, ON, Canada**

2. **Department of Neuroscience, Carleton University, Ottawa, ON, Canada**

[‡]These authors contributed equally to these experiments.

***Correspondence should be addressed to E.M.M., M.C.D., and M.R.H. (maria.derosa@carleton.ca, emcconn2@connect.carleton.ca, and matthew.holahan@carleton.ca)**

Article keywords: DNA aptamer, targeted delivery, liposome, blood-brain barrier, dopamine, SELEX

Abstract

The delivery of therapeutics across the blood-brain barrier remains a considerable challenge in investigating central nervous system related processes. In this work, a liposome vehicle was surface-modified with an aptamer that binds to the transferrin receptor and was loaded with two different dopamine-binding aptamer payloads. This system was effectively used to promote the delivery of the aptamer cargo from the peripheral injection site into the brain. The effect of these delivered aptamers on behaviour was investigated *in vivo* in a locomotor task. The first dopamine binding aptamer assessed was a DNA aptamer, the binding of which had been previously validated through the aptamer-based biosensor development reported by several independent research groups. The second aptamer investigated was the result of a novel *in vitro* selection experiment described herein. Our data suggest that systemic administration of the modified liposomes led to delivery of the dopamine aptamers into the brain. Fluorescence microscopy revealed differential distribution of fluorescence based on the presence or absence of the transferrin receptor aptamer on the surface of fluorescently modified liposomes. In a behavioral experiment using cocaine administration to induce elevated concentrations of neural dopamine, systemic pre-treatment with the dopamine aptamer-loaded liposomes reduced cocaine-induced hyperlocomotion. Multiple controls including a transferrin-negative liposome control, and transferrin-positive liposomes loaded with either a non-binding, base-substituted dopamine aptamer or a random oligonucleotide were investigated. None of these controls altered cocaine-induced hyperlocomotion. Chronic systemic administration of the modified liposomes produced no deleterious neurobehavioral or neural degenerative effects. Importantly, this work is one example of an application for this versatile multi-aptamer payload/targeting system. Its application general application is limited only by the availability of aptamers for specific neural targets.

Introduction

Aptamers are short, single stranded DNA or RNA oligonucleotides, typically less than 100 bases in length, which exhibit unique three-dimensional structures capable of binding targets ranging from small molecules to whole cells.[1] Aptamers are selected by an iterative *in vitro* screening process termed Systematic Evolution of Ligands by EXponential enrichment (SELEX) and can be chemically synthesized on a large scale with a high degree of reproducibility.[2–4] As such, they are relatively inexpensive and neither animals nor cell cultures are required for their production. Moreover, aptamers are reversibly denaturable and have extended shelf lives.[5] They exhibit long *in vivo* half-lives (hours to days) when properly modified, are nontoxic and exhibit low immunogenicity.[6,7] For these reasons, aptamers have many potential analytical, diagnostic, and therapeutic applications.[5]

An important characteristic underlying the success of diagnostic and therapeutic protocols based on aptamer technology lies in the ability of the aptamer to bind to its target with high affinity and selectivity (discriminating between closely-related molecules), exhibiting binding properties comparable to monoclonal antibodies.[5,7] High specificity, increased affinity, ability to be therapeutically controlled, and good safety margins make aptamers optimal therapeutic and detection candidates.[8–10] Further, an advantage of aptamers over traditional therapeutics is that the complementarity of nucleic acids naturally provides each aptamer with its own antidote. This is especially beneficial for therapies associated with high risk complications, such as anticoagulation.[11] The potential of aptamers as molecular recognition elements for diagnostic and therapeutic applications within the central nervous system was previously reviewed.[12–14]

An RNA aptamer for dopamine (DA) with a moderate binding affinity was reported in the late 1990s.[15] More recently, DeRosa and colleagues developed the DNA homolog of this RNA aptamer sequence which exhibited improved binding affinity and stability over the RNA sequence, and was found to target DA and norepinephrine simultaneously.[16] Injection of this aptamer, referred to as DBA (dopamine binding aptamer), into the nucleus accumbens reversed a dopamine-dependent increase in behavioral perseveration to control levels suggesting that the aptamer, when injected directly into the brain, bound to DA and to some degree norepinephrine, rendering those neurotransmitters unable to activate postsynaptic targets.[17]

While targeted intra-cranial injections of aptamers represent a huge step in not only basic research but also preclinical investigations, designing a strategy to deliver the aptamer across the blood-brain barrier (BBB) and investigating its effects on neurobehavioral function are essential steps in the development of novel therapeutic compounds for central nervous system disorders. The objectives of the present study were to provide proof-of-concept for the development of a multi-aptamer payload/targeting system for delivery of an aptamer across the blood brain barrier. This multi-aptamer payload/targeting system may present novel therapeutic potential as well as diagnostic and analytical research value.

An effective strategy for the delivery of nucleic acids to the brain exploits receptor mediated transcytosis to carry a loaded vehicle across the BBB, an approach coined as a "Molecular Trojan Horse".[18–22] Liposomes, spherical vesicles consisting of one or more lipid bilayers enclosing aqueous compartments, have been widely investigated for the past forty years as carriers to improve the delivery of therapeutic payloads, including nucleic acids to specific sites in the body.[23–26] Aptamers have been conjugated to the surface of liposomes for the effective specific delivery of their payload, such as anti-cancer drugs, and have been shown to

improve specific cellular uptake and toxicity.[27] In the context of delivery to the brain, this has been attempted by modifying liposomes with a recognition element, typically monoclonal antibodies, capable of targeting transferrin receptors to increase their access through the BBB by receptor or absorptive-mediated transcytosis.[19] Transferrin receptors are highly expressed on endothelial cells, components of the BBB and the blood cerebrospinal fluid barrier, and are known to be involved in transport of their ligand, transferrin across these brain barriers.[28–30] Strategies to specifically deliver cargo to the brain via receptor mediated transcytosis across the BBB have exploited the role of transferrin and the transferrin receptor by conjugating either transferrin, or an anti-transferrin receptor antibody to the surface of a nanoparticle, such as an immunoliposome, or directly to another antibody.[21,31–34] In fact, oligonucleotide cargo has been delivered to the brain in this manner.[35]

Given the practical advantages that aptamers have in terms of cost and ease of synthesis, as well as the promise that aptamers hold for diagnostic and therapeutic applications in the CNS, an aptamer-based modification of the Molecular Trojan Horse, where both the targeting agent and the payload (DBA) were aptamers, was investigated in the present work. The targeting agent chosen was a transferrin receptor DNA aptamer (TRA), which was conjugated to the surface of aptamer-loaded liposomes in this study. This aptamer was previously selected by Chen et al (2008) to bind to the extracellular domain of the mouse transferrin receptor.[36] The transferrin binding domain of the TRA has been well characterized.[37,38] The ability of the TRA to specifically activate the transferrin receptor and induce cellular internalization compared to mutant aptamer controls has been shown in mouse fibroblasts, B16 cells (melanoma) and bEND5 cells (*in vitro* BBB model).[36,37,39,40] Additionally, a minimized version of the TRA was shown to transcytose the BBB in a NOD/SCID mice.[41]

Results & Discussion

Selection of the novel dopamine binding aptamer DA20m

Both the RNA dopamine binding aptamer originally selected by Mannironi et al., and the DNA homolog (DBA) showed good affinity for dopamine, with dissociation constants of 1.6 ± 0.2 μM and 0.7 μM respectively, however these aptamers exhibited some affinity for the neurotransmitter norepinephrine.[15,16] In fact, the DBA exhibited a slightly better affinity for norepinephrine (0.4 μM) than for dopamine. In this study, the Systematic Evolution of Ligands by EXponential enrichment (SELEX) method was used to obtain a novel DNA aptamer for dopamine.[2,4,15,42] After four rounds of affinity chromatography-based selection using a dopamine-agarose column, aptamer candidate sequences were identified by molecular cloning and Sanger sequencing. Selections for small molecules can be particularly challenging due to methodological limitations imposed by the small molecular target.[43,44] To achieve a balance between good secondary structure representation and the limitations of practical synthesis, a moderately sized selection template of 96 bases, where the random region was 60 bases long, was chosen.[44,45] The best aptamer from the candidates identified was truncated to yield the minimer aptamer, DA20m. Since both the RNA and DBA aptamers were predicted to form two stem loops which came together to form a dopamine binding pocket, the secondary structure of DA20m was examined. The secondary structure of DA20m was predicted using RNAStructure and is shown in Figure S1A.[46] The predicted secondary structure was similar to that of both the RNA and DBA aptamers in that it had three stem loop domains (alternatively described as a 3-way junction), however the middle and 3'-domains contained fewer base pairs and would therefore be theoretically less stable than the RNA and DBA binding aptamers respective domains.[15,16,47] Aptamers tend to have high G and C content and consequently the G-quadruplex is a common secondary structure.[48–51] To determine if the DA20m aptamer may

form a G-quaruplex rather than a three-way junction, the base composition of the DA20m aptamer sequence was examined (Figure S1 B) and its ability to form a G-quadruplex was predicted using QGRS Mapper.[52,53] Two possible G-quadruplex regions were identified (see supplemental Table S1). Thermal denaturation was used to examine the secondary structure in both the presence and absence of dopamine. By this method, the secondary structure was determined to exhibit more duplex, rather than G-quadruplex character (indicated by the lack of hyperchromicity observed at 295 nm with increasing temperature in Figure S2). Finally, the affinity of the DA20m aptamer for dopamine was evaluated using fluorescence anisotropy (Figure S3). The apparent dissociation constant was determined to be 0.11 ± 0.08 μM.

Multiple sensors for the detection of dopamine have been developed using either the RNA or DNA DBA.[54–86] In one instance, both the DNA and RNA aptamers were investigated in the same platform and the DNA homolog aptamer showed increased sensitivity and specificity.[87] Since the binding affinity and selectivity of the DBA has been well characterized by several independent research groups, the DBA was investigated as the main aptamer of interest in this work and the novel aptamer selected in this work was used to validate the generality of the system.

Design and synthesis of dopamine aptamer-loaded, transferrin receptor aptamer-modified (DAL-TRAM) liposomes

Delivery across the BBB is a persistent challenge in the development of new therapeutics targeted to the brain. Only a minor class of drugs can actually cross the BBB: lipid soluble molecules of less than 400 Da in size. Large molecule therapeutics such as recombinant proteins, siRNAs and non-viral gene medicines cannot cross the BBB.[20] Aptamers, being relatively

large (~10-15 KDa), charged, polar molecules, are no exception. Although some work has been done to specifically select aptamers that cross the blood brain barrier, and recently RT-qPCR has shown that low levels of systemically administered aptamer has been detected in the brain, the development of vehicles for efficient BBB passage remain an important goal.[28,88]

The biocompatibility and biodegradability of liposomes has been extensively demonstrated and characterized, therefore liposome were selected as the delivery vehicle for the multi-DNA aptamer based payload/targeting system.[25] PEGylated liposomes were used in this payload/targeting design as inclusion of the polyether polyethylene glycol (PEG) has been shown to increase circulation time. Consequently, this design is not only an effective delivery modality but is cost effective, and easily transferable to mass production.[23] Given the chemical and physical properties of liposomes (stability, ease of synthesis and surface modification, and batch-to-batch reproducibility),liposomes were especially compatible with aptamers for the development of targeted delivery systems for the central nervous system. In fact, the clinical use of several liposome-based drug delivery systems to treat disease has been approved by the FDA..[27,89,90]

Inspiration for the design of the DAL-TRAM liposomes examined in this research came from work done by Shi et al., 2001.[18] In that work, monoclonal transferrin receptor antibodies were conjugated to PEGylated liposomes containing plasmid DNA. By this strategy, the peripherally administered “Molecular Trojan Horse” formulation was transported across the BBB. Further, this particular liposome formulation was chosen as these anti-transferrin receptor monoclonal antibody modified liposomes had previously been shown to exhibit stability in blood and had been successfully used to delivery of an exogenous gene to the brain.[19] Additionally, PEG-stabilized immunoliposomes composed of the same lipids used in the study presented

herein, were shown to be size-stable in 50 mM HEPES buffer (pH = 7.0) at room temperature for at least 24 days.[91] Importantly, DNA encapsulation remained constant for at least 48 hours in both 50 mM HEPES buffer (pH=7.0) at room temperature as well as in Dulbecco's Modified Eagle's Medium (DMEM: used to model *in vivo* conditions), at 37°C for at least 48 hours.[91]

In the current study, aptamers were used as both the transport mediator and payload. The schematic design of the multi-aptamer payload/targeting system is shown in Figure 1A.

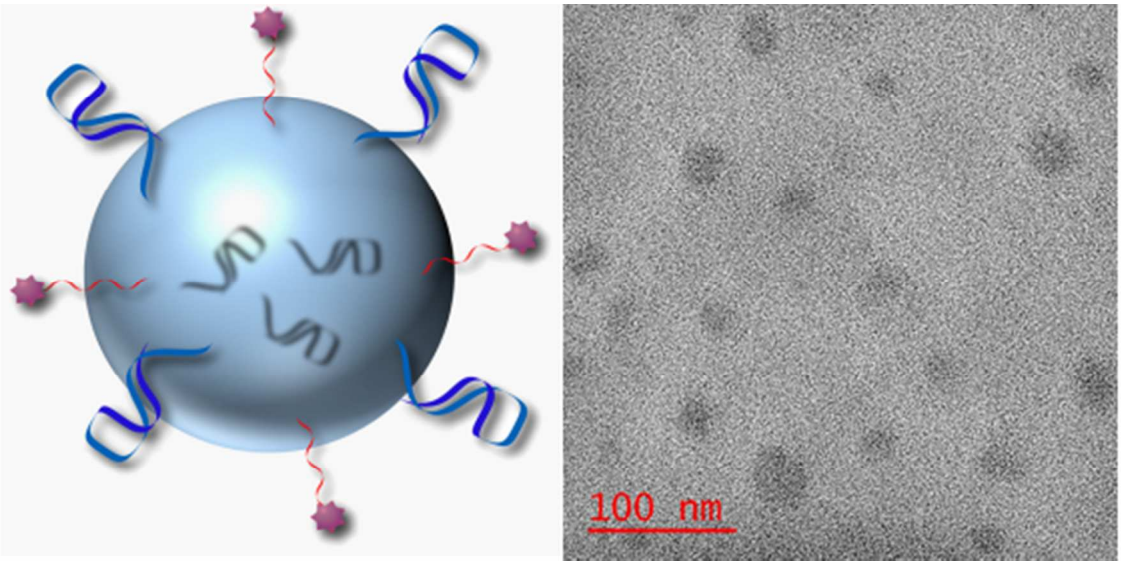

Figure 1: A) Schematic of the multi-aptamer payload/targeting system. The blue sphere represents the lipid vesicle composed of: POPC, 18:0 DDAB, 18:0 PEG 2000 PE, DSPE-PEG 2000-malemide, and either Liss Rhod PE or 16:0 NBD PE. The liposomes were loaded with payload aptamer (black ribbons), and surface modified with transferrin receptor aptamer (TRA: blue ribbons). Inclusion of a fluorescently modified lipid (represented by pink stars) allowed for fluorescent imaging of the liposome vehicle. B) Representative transmission electron microscope image of aptamer loaded-TRAM liposomes.

The payload of the TRAM delivery vehicles was either a dopamine binding aptamer (DBA), a non-binding, base-substituted dopamine aptamer control (Sub), a random oligonucleotide (ROL) or the newly selected dopamine aptamer (DA20m) (see Table 1 for more details). To allow for fluorescence imaging of the central distribution of the peripherally injected DAL-TRAM and control liposome formulation, either rhodamine or NBD-modified lipid was

included in the design. In place of monoclonal antibodies for the transferrin receptor, a thiol modified transferrin receptor aptamer (TRA) was conjugated to the surface of the liposome via a thioether bond to maleimide-modified lipid.[36]

Encapsulation within the liposomal vehicle affords protection to the unmodified nucleic acid payload. This allows the aptamer to be delivered to the brain intact and in its natural state. Alternative strategies to increase nucleic acid circulation time include 5'- and 3'- end modifications, inclusion of modified nucleotides and modifications to the nucleic acid backbone.[6,92] However, when these modifications are made post aptamer selection, they can disrupt the secondary structure of the aptamer as well as the affinity of the aptamer to its target. Further, encapsulation of the aptamer payload into the targeting liposome effectively concentrates the aptamer payload by facilitating specific delivery to the cellular target. Therefore, delivery of the unmodified oligonucleotide via encapsulation within the protective liposomal vehicle was investigated. Small, unilamellar liposomes were prepared as previously described with some notable differences, namely the incorporation of a DNA aptamer targeting moiety and encapsulation of a DNA aptamer payload.[19,93] The synthesis process is described schematically in supplemental Figure S4. Successful synthesis, lamellarity, and monodispersity of the DAL-TRAM formulation was determined by gel electrophoresis (supplemental Figure S5) and transmission electron microscopy (TEM) (Figure 1B and supplemental Figure S6). The final loaded-TRAM formulations consisted of small unilamellar liposomes with an average diameter of 57 +/- 11 nm. Additionally, the stability of liposomes in 90% human serum at 37°C was assessed by TEM imaging (see supplemental Figure S7). DAL-TRAM in 50 mM HEPES buffer (pH=7.0) was combined 1:9 with human serum. These samples were incubated at 37°C for 24 hours. At specific time points (0 min, 15 min, 30 min, 1 h, 12 h and 24 h) an aliquot of the

sample was removed and deposited on a grid for TEM imaging. Although some aggregation was observed over time, features consistent in size and shape with intact liposomes were observed at each time point. Representative images for DAL-TRAM+serum at 0 min, 1 h and 24 h are shown. The long-term stability of the liposomes (in 50 mM HEPES buffer (pH=7.0) over time was assessed by nanoparticle tracking analysis (NTA) and TEM after 2 and 5 months respectively (see supplemental Figure S8). Intact liposomes were observed by NTA after 2 months, and by TEM imaging after 5 months; however some aggregation was also observed in the TEM images. The difference in the size measured by TEM and NTA can be attributed to differences in the methods.[94] In TEM the particles are dried on a grid and their size is measured based on the diameter of the dried particle. In NTA, the particle size is measured in solution. Hydration of the particle can increase the observed radius. Additionally, the particle size is measured in 2-dimensions where as the particle moves in 3-dimensions, this can lead to an increase observed size.[94] Based on the distribution of particle sizes observed, it is also possible that aggregates of smaller particles skewed the distribution. Nevertheless, loaded-TRAMs were prepared and used within 4 days for all further experiments. A number of variations to the DAL-TRAM design, described in table 1 were also synthesized as controls. The DNA sequences used in each formulation are shown in Table S2.

Table 1: Aptamer and multi-aptamer payload/targeting system and control variation abbreviations

Abbreviation	Aptamer details
DBA	Dopamine binding aptamer
Sub	Non-binding/base substituted dopamine binding aptamer. The sequence is identical to DBA with the exception of specific point mutations, the presence of which eliminates dopamine-aptamer binding[16]
ROL	Random oligonucleotide of comparable length to the DBA previously shown not to affect dopamine-related behavior[17]
DA20m	Newly selected dopamine binding aptamer of similar size to the DBA that was used during the liposome synthesis phase as a complex secondary structure analog. To validate the generality of the delivery

	system, this aptamer was evaluated in the behavioral testing.
Abbreviation	**Component details**
DAL-TRAM	Dopamine aptamer loaded-transferrin receptor aptamer modified liposome (TRA-positive liposome)
DAL	Dopamine aptamer loaded liposome (TRA-negative liposome)
TRAM	Transferrin receptor aptamer modified liposome (no oligonucleotide payload)
Sub-TRAM	Non-binding/base substituted dopamine binding aptamer loaded – transferrin receptor aptamer modified liposome
ROL-TRAM	Random oligonucleotide loaded-transferrin receptor aptamer modified liposome
DA20m-TRAM	DA20m aptamer loaded-transferrin receptor aptamer modified liposome (TRA-positive liposome)

Detection of DAL-TRAM in the Brain

The central distribution of peripherally administered DAL-TRAM and DAL were qualitatively assessed by fluorescence microscopy. Mice (n=3) were injected (0.15 mL) with an equimolar combination of TRA-positive DAL-TRAM (rhodamine labelled) and TRA-negative DAL (NBD labelled) liposomes prepared in 50 mM HEPES buffer (pH=7.0). Representative images from coronal sections through the nucleus accumbens are shown in Figure 2.

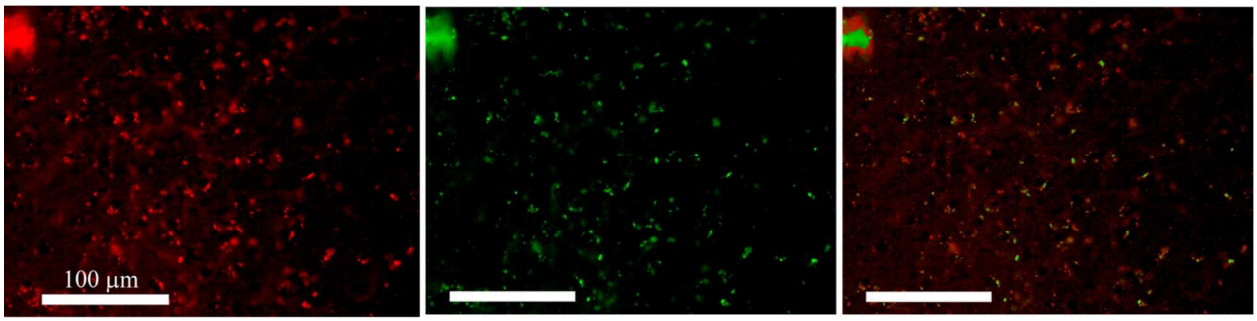

Figure 2: The distribution of rhodamine and NBD fluorescence in a coronal section (35 µm thickness) of the nucleus accumbens (20X magnification) was imaged by fluorescence microscopy. Prior to imaging, mice (n=3) were injected with an equimolar solution containing TRA-positive liposomes (DAL-TRAM: rhodamine (red) labelled) and TRA-

negative liposomes (DAL: NBD (green) labelled). The scale bars for the DAL and overlay images are the same as that shown in the DAL-TRAM image.

The fluorescent distribution of the rhodamine-labeled DAL-TRAM (Figure 2) suggests that the DBA was successfully delivered to the brain via the DAL-TRAM. When examining the fluorescent images, there was a very clear difference between the fluorescent distribution of TRA-positive DAL-TRAM (red) and TRA-negative DAL (green) liposomes. The red fluorescence of the DAL-TRAM was much more diffuse, suggesting diffusion within the interstitial space and around the cell bodies as compared to the punctate fluorescence signal of the green DAL. Based on these patterns of overlapping (red and green puncta) and non-overlapping (diffuse red) fluorescent signals, it was concluded that the DAL-TRAM diffused beyond the capillaries and into neural tissue while the TRA negative DAL did not diffuse into the neural tissue and remained trapped within the capillaries. A second imaging study was preformed to ensure that the differences in distribution observed were not due to the differences in the lipid conjugated dye used in the preparation of the DAL-TRAM and DAL formulations. Two experimental groups were examined: transferrin aptamer negative liposomes (DALs: rhodamine labeled, n=3) and transferrin aptamer positive liposomes (DAL-TRAMs, rhodamine labeled, n=3). A control group was injected with saline (n=3). Representative images from coronal sections through the nucleus accumbens are shown in Figure S9. These results were consistent with that observed for the dual colour imaging assay (Figure 2). In the TRA-negative liposome group (DAL), rhodamine was observed mostly around the capillaries, and did not seem to have significantly diffused into the interstitial space. In contrast, the distribution of the TRA-positive liposomes (DAL-TRAM) is much more diffuse. The contrast between cell bodies (black spheres) and rhodamine fluorescence (white areas) is much more obvious in the TRA-positive

(DAL-TRAM) image compared to the control liposomes (TRA-negative DAL) and saline representative images.

In addition to the fluorescence-based detection of the liposomes within the brain, direct detection of the aptamer sequences themselves were attempted using RT-qPCR (see supplemental Table S3 and Figure S10). Unfortunately, due to similarity between the aptamer sequence and mouse genomic DNA, primers could not be designed that allowed for specific, reproducible amplification of the aptamer target from tissue extract (see Table S3).[95] Additionally, since the amplicons produced by non-specific amplification were predicted using NCBI software Primer-Blast to be non-specific and of various sizes (~75-3500 base pairs), RT-qPCR amplification data was analysed using gel electrophoresis in an attempt to minimize the effect of non-specific amplification which could not be eliminated by examining the quantitation cycle alone.[96]

To determine whether the addition of TRA resulted in a significant difference in the delivery of DBA to the brain, the delivery of DBA by DAL-TRAM was compared to that of DAL (Figure S10). There was no difference between the average quantitation cycle (Cq) of DAL-TRAM (21.8 ± 0.1) and DAL (21.8 ± 1.0), suggesting the DBA is delivered to the brain by both vehicles. However, Analysis by One-way ANOVA revealed a statistically significant difference in the observed optical density between groups ($F(3,9) = 20.843$, $p<0.001$ at $\alpha=0.05$). Post-hoc analyses by Fisher's LSD revealed that the mean optical density of both the DAL-TRAM ($p<0.001$) and DAL ($p=0.003$) were significantly higher than the NTC whereas the difference between the mean optical density of DAL-TRAM (37.7 ± 3.6) and DAL (28.2 ± 1.5) approached significance ($p=0.053$ at $\alpha=0.05$). These results mirror what has been observed in a recent study attempting to select brain-penetrating aptamers using a novel *in vivo* SELEX

approach.[28] In this experiment, RT-qPCR did not reveal a statistically significant difference in concentration of the BBB-crossing sequence within separated capillary and parenchymal tissue. Given that our fluorescence microscopy data indicate that DAL appears to be primarily trapped in the capillaries it is perhaps not surprising that the DBA is detected by RT-qPCR in these controls.

Acute Systemic Aptamer Injection and Cocaine-Induced Locomotion

In order to assess the efficacy of systemically administered DAL-TRAM, several experiments were run to determine 1) the ability of an acute systemic administration of DAL-TRAM to attenuate hyperlocomotion in cocaine-treated animals 2) validation of the system with a second dopamine binding aptamer, DA20m , 3) the specificity of the DBA component of the DAL-TRAM in mitigating cocaine-induced behavioral changes, and 4) whether chronic systemic administration of DAL-TRAM produced any motor deficits or noticeable neuronal degeneration. Cocaine is known to be a potent activator of the dopamine-reward system as well as the noradrenergic and serotonergic systems.[97] Despite the significant role of dopamine in motor behaviour, this is an appropriate model to test the DAL-TRAM as the authors have shown previously that direct intra-accumbens injection of the unmodified DBA aptamer does not impair locomotion.[17] Treatment strategies for cocaine addiction and particularly, the prevention of craving and relapse are limited, and their effectiveness is still questionable.[98] Therefore, not only is cocaine a well-characterized drug for experimental purposes in the laboratory but it also has human, clinical relevancy for treatment need.

Examining the efficiency of DAL-TRAM in reducing cocaine-induced hyperlocomotion and validation of the system with DA20m-TRAM

In the first behavioral assessment mice (n = 53) were assigned to one of 7 conditions: pretreatment (i.p.) with a Sub control oligonucleotide packaged within the TRAM (Sub-TRAM) followed by an injection (i.p.) of 10 mg/mL cocaine (Sub-TRAM+10 mg/mL cocaine; n =8); pretreatment (i.p.) with DAL-TRAM followed by an injection (i.p.) of 10 mg/mL cocaine (n = 8), an i.p. injection of 5 mg/mL cocaine (n = 8), an i.p. injection of 1 mg/mL cocaine (n = 7) or an i.p. injection of saline (n = 8); pretreatment (i.p.) with an injection of TRAM containing no oligonucleotide payload followed by a saline injection (n = 8); or pretreatment (i.p.) with an injection of saline followed by saline (n = 6). Mice received their first injection (loaded-TRAM or TRAM) followed 5 minutes later by the second injection (cocaine or saline) and then 5 min later were individually placed into the locomotor apparatus for a 30 min session. Horizontal activity was recorded every 5 minutes and total locomotor activity was compared between treatment conditions. To validate the delivery system, the effectiveness of a second dopamine binding aptamer, DA20m, was assessed in a similar assay where pretreatment (i.p) with an injection of DA20m-TRAM followed by 10 mg/mL cocaine (n=8), pretreatment (i.p) with an injection of DAL-TRAM + 10 mg/mL cocaine (n=8), pretreatment (i.p) with DA20m-TRAM followed by saline (n=9), and pretreatment (i.p) with DAL-TRAM followed by saline (n=8) were compared to Sub-TRAM + 10 mg/mL cocaine (n=7) were assessed. These data are shown in Figure 3 (DBA), Figures S11-13 (cocaine controls) and Figure S14.

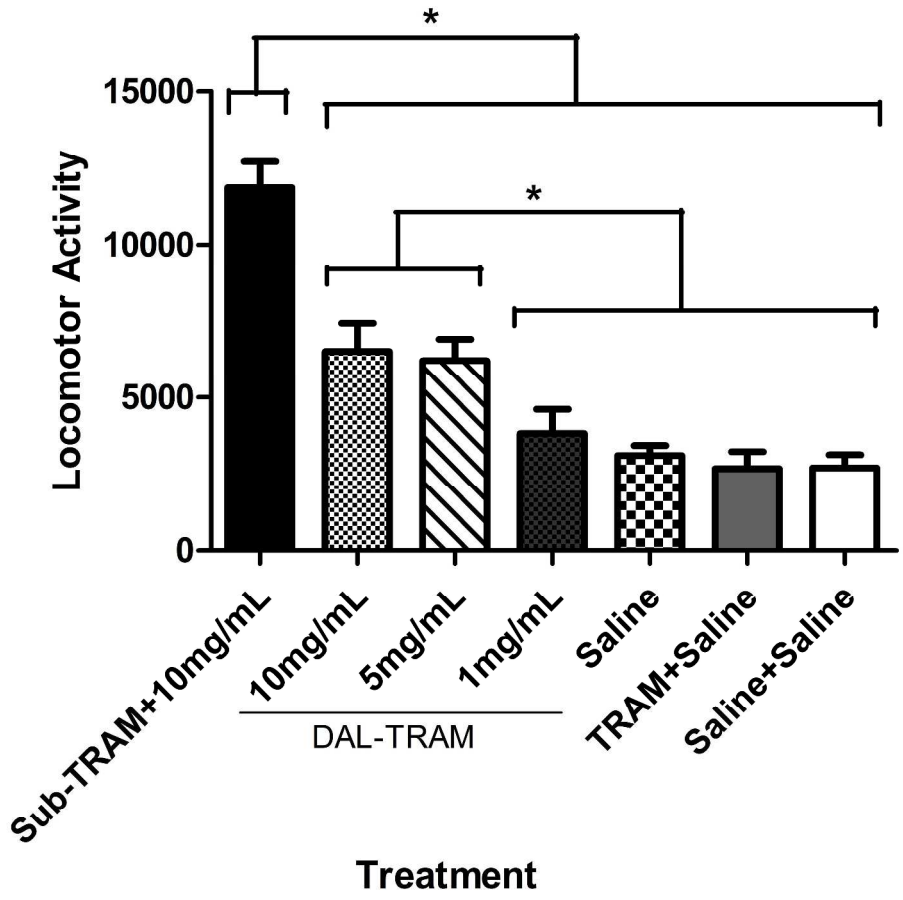

Figure 3: The ability of DAL-TRAM to reduce cocaine-induced hyperlocomotion at different cocaine doses was assessed over 30 min. The total horizontal activity recorded is shown. A significant effect of group was revealed following ANOVA ($F(6,46) = 22.71$, $p<0.001$). Significant differences between treatment conditions were revealed by Fisher's LSD post-hoc analyses as indicated (*$p < 0.05$).

One way ANOVA on the total number of activity counts during the 30 min test revealed a significant group effect ($F(6,46) = 22.71$, $p < 0.001$; Figure 3). Fisher's LSD post-hoc analyses revealed that group Sub-TRAM + 10 mg/mL cocaine was more active than all other groups ($p < 0.05$). Groups DAL-TRAM + 10 mg/mL cocaine and DAL-TRAM + 5 mg/mL cocaine were more active than groups DAL-TRAM + 1 mg/mL cocaine and the 3 saline-treated control groups ($p < 0.05$). A breakdown of activity counts per 5 min time bin for the groups

pretreated with DAL-TRAM or TRAM followed by cocaine (10, 5 or 1 mg/mL) are shown in supplemental Figures S11-S13. These data suggest that the DAL-TRAM pretreatment was effective in reducing the cocaine-induced hyperlocomotion across the entire 30 min test. To validate this system, a second dopamine binding aptamer (DA20m) with similar affinity to the DBA was evaluated for its ability to decrease cocaine-induced hyperlocomotion (Figure S14). A significant effect of group ($F(4,34) = 20.12$, $p<0.001$) on the cumulative locomotor activity over the entire 30 min session was revealed using analyses by One-way ANOVA. Significant differences between treatment groups were revealed by Fisher's LSD post-hoc analyses. A significant decrease in cumulative locomotor activity was observed for the DA20m-TRAM + 10 mg/mL cocaine treated group compared to the Sub-TRAM + 10 mg/mL cocaine treated control group ($p=0.009$). Additionally, the difference between the two aptamer groups (DAL-TRAM vs DA20m-TRAM) was not significant ($p=0.054$), as expected given the aptamers exhibited similar affinity. As with the DAL-TRAM + 10 mg/mL cocaine treated group compared to the DAL-TRAM + saline treated group, the locomotor activity of DA20m-TRAM + 10 mg/mL cocaine was significantly higher than that of DA20m-TRAM + saline ($p<0.001$). There was no difference between the DA20m-TRAM + saline, or DAL-TRAM + saline groups. These data were interpreted to suggest that the TRAM vehicle is effective at delivering aptamer cargo to the brain, and that another dopamine binding aptamer could be delivered this way to mediate locomotor behaviour. Since the novel aptamer, DA20m did not show a significant decrease in the locomotor activity compared to the DBA, additional experiments focused on the DBA given that its dopamine binding had been externally validated by several research groups.

The differences in locomotion observed between experimental and control groups can be attributed to the specific affinity of the DBA and DA20m aptamers for dopamine. Although

locomotor behaviour was not normalized to the level of the saline controls in either DBA or DA20m treated mice, overall, both the DAL-TRAM and DA20m-TRAM were effective in decreasing cocaine-induced hyperlocomotion. The reduction seen is similar to that expected from traditional D1/D2 antagonists, however the dopamine binding aptamers examined in this study are proposed to function by a different mechanism. Based on the affinity of the aptamers for free dopamine, the DBA and DA20m are thought to bind directly to synaptic DA, effectively decreasing the available concentration of DA in the synaptic cleft. By this mechanism, locomotor behaviour was nearly normalized.

Variations of the multi-aptamer payload/targeting system (DAL-TRAM) were assessed for specificity

To examine the possible effects of the non-active components of the multi-aptamer payload/targeting system on cocaine induced hyperlocomotion, several controls were examined and compared to DAL-TRAM. The following control (saline treated) and experimental (10 mg/mL cocaine treated) groups were examined: saline/saline (n=6), TRAM/saline (n=8), DAL-TRAM/saline (n=8), DAL-TRAM/cocaine (n=8), DAL/cocaine (n=9), ROL-TRAM/cocaine (n= 7), TRAM/cocaine (n= 8), and Sub-TRAM/cocaine (n=8). Mice received their first injection (loaded-TRAM variation) and then 5 minutes later received the second injection (cocaine or saline). After a 5 min delay, mice were placed into the locomotor apparatus for a 30 min session. Horizontal activity over the 30 min session was compared between the treatment conditions (Figure 4).

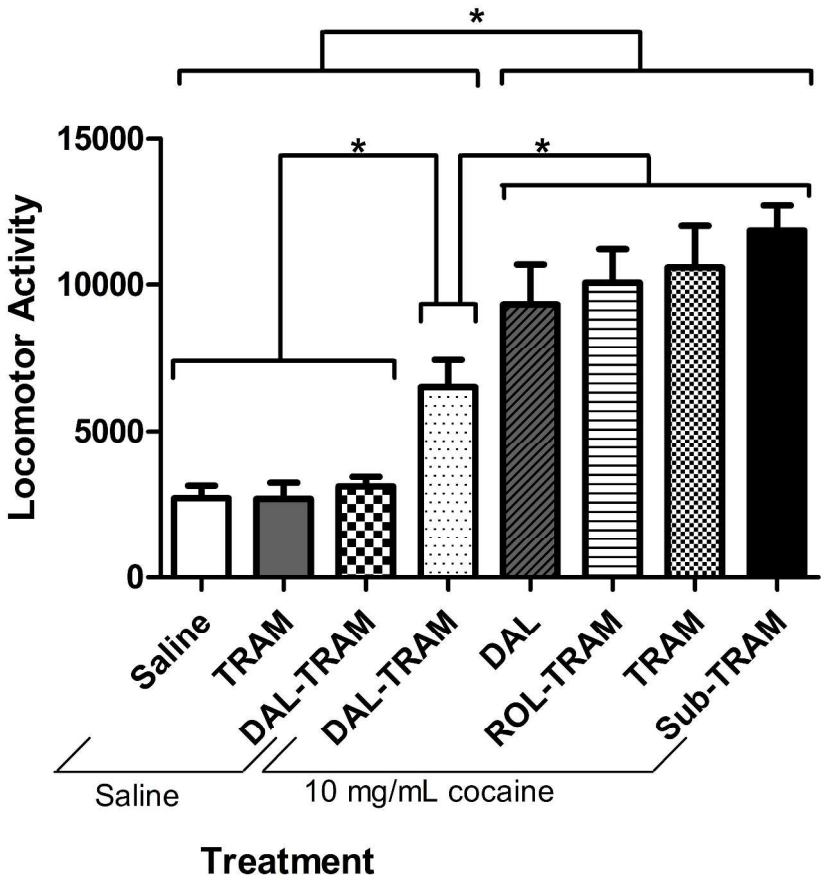

Figure 4: The specific efficacy of the multi-aptamer payload/targeting system in cocaine-induced hyperlocomotion was evaluated by comparing its action to multiple system variations. Total horizontal activity is shown. A significant group effect was revealed by one-way ANOVA ($F(7,54) = 14.22$, $p < 0.001$). A significant difference between groups was revealed by Fisher's LSH post-hoc analyses (*$p < 0.05$).

A One way ANOVA on the total number of activity counts during the 30 min test revealed a significant group effect ($F(7,54) = 14.22$, $p < 0.001$;Figure 4). Fisher's LSD post-hoc analyses revealed a significant difference between the DAL-TRAM/cocaine group and all other groups ($p<0.05$). The DAL/cocaine, ROL-TRAM/cocaine, TRAM/cocaine and Sub-TRAM/cocaine groups all showed significantly elevated locomotor activity compared to both the aptamer (DAL-TRAM/cocaine; $p<0.05$)) and saline control groups ($p<0.001$). These data

suggest that the TRA mediated delivery of the DBA payload was responsible for the observed decrease in hyperlocomotion. A reduction in hyperlocomotion was only observed when the multi-aptamer payload/targeting system (DAL-TRAM) was intact. When the payload (DBA) was administered in the absence of the targeting moiety (TRAM) via the DAL liposome, no significant reduction in hyperlocomotion was observed. Therefore, even when the aptamer was administered systemically, it was not delivered to the brain without the TRAM component of the system. Additionally, the non-specific effect of a random oligonucleotide (ROL-TRAM) or a non-binding variant of the DBA (Sub-TRAM) on hyperlocomotion were examined and no significant reduction in hyperlocomotion was observed in either case. Therefore, the presence of foreign DNA alone was not responsible for the observed decrease in locomotor behaviour in cocaine treated animals. Finally, when the TRAM liposome was administered with no payload, no significant reduction in hyperlocomotion was observed.

Importantly, the significant decrease in locomotor behaviour of the DAL-TRAM/cocaine treated animals compared to the transferrin-negative liposomes (DAL/cocaine)), random oligonucleotide (ROL-TRAM/cocaine), non-binding DBA variant (Sub-TRAM/cocaine) and the liposome with no oligonucleotide payload (TRAM/cocaine) suggested the DBA was solely responsible for the observed decrease in locomotor behaviour. Moreover, acute treatment with the DAL-TRAM/saline did not produce significant motor deficits in saline treated animals compared to saline/saline treated animals. Consistent with our previously published data, this is an important advantage of the multi-aptamer payload/targeting system, specifically the DBA over traditional D1/D2 antagonists, as these therapeutics often cause disruptive extrapyramidal side effects.[99]

Chronic administration of DAL-TRAM in saline treated animals

Horizonal movement was recorded directly following treatment with DAL-TRAM (n= 5), TRAM (n= 5) or no injection (n= 5), each day for six days. Statistical analysis by one-way ANOVA revealed no main effect of group on total locomotor activity ($F(3,24)=0.949$, $p=0.433$). Recorded values of horizontal movement for each treatment group, on the last day (day 6) are shown in Figure 5. Additionally, a daily record of horizontal movement for each 5 min time bin, for each treatment condition is shown in supplemental Figure S15. These data suggest that locomotor activity is not affected by chronic DAL-TRAM or TRAM administration.

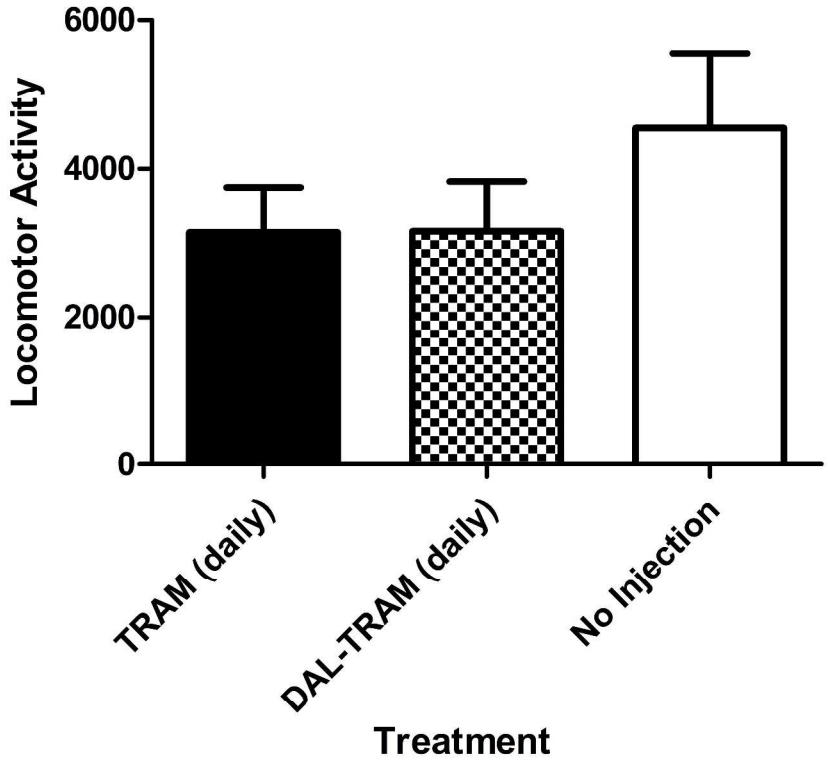

Figure 5: No effect on motor behaviour was observed after chronic administration of DAL-TRAM, in the absence of cocaine. The total horizontal activity recorded during the final 30 min session of the experiment is shown. Statistical analysis by one-way ANOVA revealed no significant group effect ($F(3,24)=0.949$, $p=0.433$).

With preliminary evidence to suggest that acute injection of the DAL-TRAM did not produce motor deficits in saline treated animals, further experiments were initiated to determine if chronic injection of either the DAL-TRAM/saline or the TRAM/saline would produce motor deficits (Figure 5). These groups were compared to the locomotor activity of a no injection group. There were no significant motor deficits observed for either experimental group suggesting chronic systemic administration of neither DAL-TRAM nor TRAM produces locomotor consequences.

Investigation of neuronal degeneration by Fluoro-Jade B Staining

Potential cellular damage following chronic administration of either DAL-TRAM or TRAM was assessed using Fluoro-Jade B staining forty-eight hours after the last locomotor assessment..[100] Images of stained tissue were acquired from the DAL-TRAM, TRAM and no injection groups and subsequently compared to images of control tissue obtained from a published report. In the control image, visible damage had been caused by implantation of a chronic, indwelling cannulae (Figure 6).[100,101] Extensive Fluoro-Jade B staining of the Positive control, which originated near the cannula tip and extended outward was likely due to neuronal damage, and reactive astrocytes or gliosis. Damaged neurons stained by Fluoro-Jade B in the positive control (Figure 6 A) are indicated by white arrows (A). In comparison, no evidence of degeneration or damage by Fluoro-Jade B staining following chronic administration of the DAL-TRAM (B) and the TRAM (C). The staining patterns of these images appeared most similar to the negative, no injection control (D).

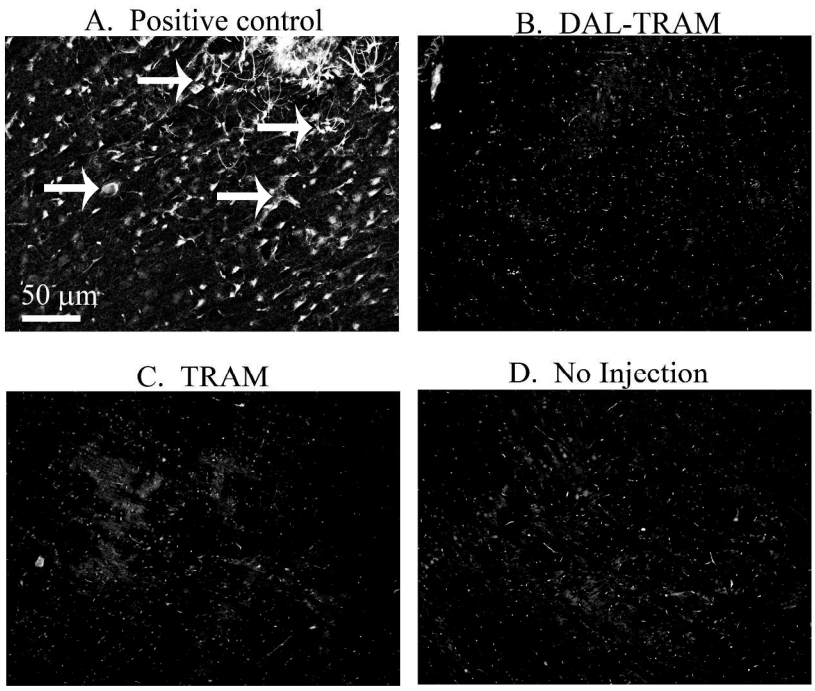

Figure 6: No indication of neural damage was observed following Fluoro-Jade B staining in animals that had been chronically treated with DAL-TRAM (B), TRAM (C), or were given no injection (D). Regions of neural damage in the control image (A) are indicated by white arrows. Magnification is at 20X.

Fluoro-Jade B is known to stain the cell bodies, axons, axon terminals and dendrites of degenerating neurons with high affinity and results in minimal background staining regardless of the source or mechanism of injury.[100,102] As an initial indication of cellular viability following chronic administration of either DAL-TRAM or TRAM, no sign of cellular damage after repeated injections was observed in the nucleus accumbens. Future experiments are

necessary to more thoroughly investigate early indications of inflammation and cellular damage.[103]

Results of the experiments performed in this study have shown that the multi-aptamer payload/targeting system, DAL-TRAM, described is effective in decreasing cocaine-induced hyperlocomotion without causing motor side effects or cellular damage. Given the results of our previously published data, it is feasible this system with the particular DBA payload is not only to cocaine addiction but that it could help normalize cognitive deficits associated with schizophrenia as well.[17] This is an especially important development as, to the authors' knowledge these data presented here demonstrate the first example of an IP delivered multi-aptamer payload/targeting system to cross the BBB and successfully attenuate behaviour in an animal model of mental illness-associated behaviours. The potential of this multi-aptamer payload/targeting system is limited only by the availability of aptamers for specific targets within the CNS. Neither is the functionality of the aptamer limited; currently applications of aptamers within the CNS include but are not limited to diagnostics, therapeutics, contrast and imaging agents, receptor modulators etc.[12] Additionally the incorporation of modified aptamers such as SOMAmers and aptazymes could expand the target diversity as well as add additional elements of structural stability, biostability and functionality to the multi-aptamer payload/targeting system.[104,105] Future work will examine modifications to this system to optimize it for more generalized CNS treatment approaches. For example, changes to the TRA targeting moiety of the multi-DNA aptamer payload/targeting system will be investigated. Recently, a truncated version of the originally reported TRA as well as rationally designed full length mutations were reported that showed increased structural stability and biological activity compared to the TRA investigated in this work.[37] The combination of aptamer modifications for increased *in vivo*

stability and circulation time post liposome release as well as optimization of the properties of the payload/targeting liposomal system to enhance therapeutic efficacy by means of increased payload release from the liposome vehicle will be explored.

Materials and Methods

Chemicals and reagents for liposome preparation

All DNA synthesis reagents and modifiers were purchased from Glen Research (Sterling, VA). Synthesis columns were purchased from BioAutomation (Irving, TX). Urea, ammonium persulfate, TEMED, HEPES, EDTA, Boric Acid and Tris were purchased from BioShop Canada (Burlington, Canada). 1-palmitoyl-2-oleoyl-sn-glycero-3-phosphocholine (16:0-18:1 PC, POPC), dimethyldioctadecylamonium bromide salt (18:0 DDAB), 1,2-distearoyl-sn-glycero-3-phosphoethanolamine-N-[methoxy(polyethylene glycol)-2000] (ammonium salt) (18:0 DSPE-PEG 2000 PE), 1,2-distearoyl-sn-glycero-3-phosphoethanolamine-N-[malemide(polyethylene glycol)-2000] (ammonium salt) DSPE-PEG 2000-malemide, Liss Rhod PE (1,2-dipalmitoyl-sn-glycero-3-phosphoethanolamine-N-(lissamine rhodamine B sulfonyl) (ammonium salt)), 16:0 NBD PE (1,2-dipalmitoyl-sn-glycero-3-phosphoethanolamine-N-(7-nitro-2-1,3-benzoxadiazol-4-yl) (ammonium salt)), mini extruder, 100 nm polycarbonate membranes and filter supports were purchased from Avanti Polar Lipids, Inc (Alabaster, AL). Slide-A-Lyser G2 dialysis cassettes were purchased from Thermo Fisher Scientific Canada (Nepean, Canada). Cocaine (ecgonine methyl ester benzoate HCl) and saline solution (0.9% sodium chloride) were purchased from Sigma-Aldrich Canada (Oakville, Canada).

Oligonucleotide Preparation

Standard phosphoramidite chemistry was performed on a MerMade DNA synthesizer (Bioautomation, Irving, TX) to prepare the oligonucleotides shown in Table 2. DNA was purified by polyacrylamide gel electrophoresis prior to molecular weight confirmation by ESI-MS.

Table 2: Sequences of oligonucleotides

Oligonucleotide	Sequence (5'→3')	Notes
Unmodified Dopamine Binding Aptamer (DBA)	GTCTCTGTGTGCGCCAGAGACACTGGGGC AGATATGGGCCAGCACAGAATGAGGCCC	
5'-thiol (Thiol-modifier C6 S-S) modified TRA	GAATTCCGCGTGTGCACACGGTCACAGTT AGTATCGCTACGTTCTTTGGTAGTCCGTT CGGGAT	
Unmodified Substituted DBA control (Sub)	GTCTCTGTGCCAAACAGAGACACTGGGG CAGATATGGGCCCGCACAGAATCCGGCC C	base substitutions corresponding to the DBA made to eliminate binding are underlined[16]
Random Oligonucleotide (ROL)	AGAATCTGTCGGGCTATGTCACTAATACT TTCCAAACGCCCCGTACCGATGCTGAACA	
DA20m aptamer	AGCGGGAGGATATGCTCTGCTGTTGGATA GGTGTATATGTGGAGATAGTAAGTGCAA TCT	

Identification of DA20m aptamer by SELEX

The DA20m aptamer is a minimal aptamer that was identified following the selection of dopamine binding aptamers from a selection library with the following template: 5'-ATACCAGCTTATTCAATT-N_{60}-AGATAGTAAGTGCAATCT-3', where N_{60} represents the number of randomized nucleotides.[15,42] Briefly, aptamers candidates were identified upon the completion of four rounds of selection using the affinity chromatography method and a dopamine-agarose column (BioRad, Saint-Laurent, QC, Canada). The selection buffer contained 50 mM Tris-HCl pH 7.4, 5 mM $MgCl_2$, 0.5 M NaCl and 0.02% L-ascorbic acid. Round-by-round enrichment was monitored by fluorescence spectroscopy where the intensity of the fluorescein modified library was measured using excitation and emission wavelengths of 490 nm and 520 nm respectively). Before each round, the enriched library was amplified by PCR by combining

2X PCR buffer (0.2 M Tris-HCl pH 9, 0.1 M KCl, 2% triton X-100) with 3.8 µL of 15 mM MgCl2, 2 µL of dNTP mix, 0.5 µL of each of the forward and reverse primers, 1 µL of TAQ DNA polymerase, 41.2 µL of deionized water and 1 uL of either the pool, control DNA (positive control) or deionized water (negative control) using the following thermal profile: 94°C for 10 min then either 30 or 45 cycles of 94.0°C (1 min), followed by 47.0°C (1 min) then 72.0°C (1 min). After the final cycle was complete, the reactions were held at 72.0°C (10 min), then cooled to and held 4°C. Aptamer candidate sequences were identified using traditional cloning and sequencing methods. Initially, the affinities of aptamer candidates were screened using fluorescence anisotropy.[106] The top aptamer candidate DA20 was identified based on sequence abundance and affinity. The sequence was arbitrarily truncated and potential minimers were screened by fluorescence anisotropy. The best minimal aptamer, DA20m, had the lowest apparent dissociation constant, and was therefore chosen to be examined in this work.

DA20m aptamer characterization

The secondary structure of the DA20m was predicted using RNAStructure by inputting the DNA sequence, setting the nucleic acid parameter to DNA, and leaving all other parameters at deault.[46] The presence of possible G-quadruplex domains were identified using QGRS Mapper.[52] Thermal denaturation profiles were obtained as previously described using a Cary 300 Bio UV-Visible spectrophotometer (Agilent, Santa Clara, CA, USA) equipped with a Cary Temperature Controller (Agilent) running the Cary Win UV Thermal application software (Version 3.00 (1.820).[107] The absorbance was measured at 295 nm over the temperature range of 20°C to 80°C using a ramp rate of 5°C/min.

Liposome Preparation

Liposomes were prepared as previously described with some important modifications[19,91,93] Briefly, POPC (19.2 μmol), DDAB (0.2 μmol), DSPE-PEG 2000 (0.4 μmol), Liss Rhod PE (0.2 μmol) and DSPE-PEG 2000-malemide (30 nmol) were dissolved in chloroform in a 10 mL round bottom flask. 16:0 NBD PE (0.2 μmol) in place of Liss Rhod PE was used for the purpose of dual-colour fluorescent imaging. The flask was capped with a septum and chloroform was evaporated off while shaking and under a flow of argon to produce a thin uniform lipid film. The lipid film was hydrated with 0.2 mL of 50 mM tris-HCl (pH=7.0) and then vortexed for 30 min. Following hydration, the flask was stored under argon and sonicated in a bath sonicator at room temperature for 10 minutes. 38 nmol of either DBA, Sub or ROL were added in a volume of 0.2 mL (50 mM Tris-HCl). The DNA was encapsulated by slowly adding 0.6 mL of 67% ethanol (to yield a final concentration of 40% ethanol). Samples were again stored under argon before being subjected to 10 cycles of 5 min in an ethanol/dry ice bath followed by 2 min in a 40°C water bath. Samples were subjected to 25 passes through 100 nm polycarbonate membranes contained in a mini-extruder. The samples were dialysed into 50 mM HEPES buffer (pH=7.0) overnight to remove the ethanol using Slide-A-Lyser cassettes (20 000 MWCO). DNA that was non-specifically interacting with the exterior of the liposome was removed via nuclease digestion. Samples were dialysed into 50 mM HEPES buffer (pH=7.0) overnight to remove the digested DNA. The disulfide bond protecting the thiol modified transferrin receptor aptamer (TRA) was cleaved in 50 mM Tris-HCl (pH=8.4) containing 100 mM DTT. The TRA was purified using biospin columns, and was buffered exchanged into 50 mM HEPES (pH=7.0) containing 7 mM EDTA. The liposomes and TRA were allowed to react for 2 hours at room temperature with gentle shaking. The samples were then dialysed overnight into 50 mM HEPES buffer (pH=7.0) to remove EDTA and unreacted TRA. Using the Stewart

Assay, it was determined that the liposome solutions generally contained a concentration of approximately 6 mg/mL of total lipids; this translates to 0.6 mg of total lipid per 100uL injection. To determine the number of liposomes delivered per injection, a theoretical calculation reported by Montanari, J., Bucci, P., and Alonso, S. was used.[108] From this calculation, it was determined that per 100uL injection, approximately 3.00×10^{13} liposomes were delivered. To maintain consistency between separate sample preparations, the liposome concentration was characterized via UV-Vis spectroscopy. The approximate concentration of the DAL-TRAM stock preparation was determined by measuring the rhodamine peak (570 nm) absorbance of a 1 in 100 dilution of the stock preparation. Rhodamine peak absorbance values of the 1 in 100 dilution of ~0.05 was assigned as 1X concentrations. Liposome sample homogeneity was characterized by TEM microscopy. Aptamer encapsulation and liposome stability over time were confirmed by gel electrophoresis and, TEM and NTA respectively. *In vitro* liposome characterization was done with liposome preparations in 50 mM HEPES buffer (pH=7.0) unless otherwise stated. Experimental details are provided in the supplemental information.

Stability of DAL-TRAM in human serum

To assess the stability of DAL-TRAM in human serum, DAL-TRAM in 50 mM HEPES buffer (pH=7.0) was combined in a 1:9 ratio with human serum, effectively diluting the liposme 1 in 10 in human serum. Pooled human male AB plasma serum was obtained from Sigma-Aldrich (Oakville, Canada). Both the DAL-TRAM and serum had been pre-warmed to 37°C. At each time point a small aliquot was removed and deposited on a grid for TEM imaging as described in the supplemental details. Between time points, the liposomes in serum were incubated at 37°C. Time points examined were at 0 min, 15 min, 30 min, 60 min, 6 h, 12 h and 24 h.

Fluorescent Detection of DAL-TRAM in the Brain

To provide an initial, qualitative assessment of DAL-TRAM entry into the brain, mice were injected (0.1 mL i.p.) with either the Rhodamine-labeled DAL-TRAM (TRA-positive liposome; n=3), Rhodamine-labeled DAL (TRA-negative liposome; n=3) or saline (n=3). Five minutes later, mice were rapidly decapitated and brains were removed then immersion fixed in 4% paraformaldehyde in 0.1 M phosphate buffer (pH 7.4). In a second experiment, mice (n=3) were injected (0.15 mL i.p.) with equimolar Rhodamine-labeled DAL-TRAM (TRA-positive liposome) and NBD-labeled DAL (TRA-negative liposome). The concentration of each liposome preparation was estimated using the extinction coefficients for rhodamine (95 000 M^{-1} cm^{-1} at 560 nm) and NBD (13 000 M^{-1} cm^{-1} at 458 nm).[109] The excitation and emission wavelengths for Liss Rhod PE and NBD PE respectively, were 560 nm/583 nm and 460 nm/535 nm. Imaging experiments were done at 1X concentration. Mice were rapidly decapitated 10 minutes following the injection. Brains were removed then immersion fixed in 4% paraformaldehyde in 0.1 M phosphate buffer (pH 7.4). Tissue was not perfused. All tissue was stored at 4° C for 24 hours, then stored in 30% sucrose/ 0.1 M phosphate (pH 7.4) at 4° C for a minimum of 72 hours.

Brains were sectioned on a cryostat (35 μm) through the nucleus accumbens (anterior posterior plane of the Paxinos and Watson atlas: 2.20 – 1.0 mm from bregma). Tissue sections were mounted on glass slides and coverslipped with Fluoromount. Using an Olympus BX61 microscope (Olympus Canada Inc., Richmond Hill, Canada), digital images of the nucleus accumbens were obtained (20x). Distribution of the rhodamine and NDB fluorescence was visualized by applying red (594 nm) and green (488 nm) filters during imaging. The exposure time was set to 350 ms for both fluorescent channels during imaging to minimize background fluorescence.

Behavioural testing and histochemical analysis

Subjects

Male CD-1 mice (32 – 38 days old) were purchased from Charles River (St. Constant, Canada) and housed individually in 27 x 21 x 14 cm clear, polycarbonate cages. The vivarium temperature (19 – 22 ºC) and humidity (50 – 60%) were controlled in a fixed range while lighting (12 hour dark/ light cycle, lights on at 08:00) remained on a constant cycle. Purina mice chow and water were available *ad libitum*. All animal procedures were approved by the Carleton University Animal Care Committee in accordance with guidelines set by the Canadian Council on Animal Care (CCAC).

Apparatus

Locomotor assessment took place in enclosed 48 x 26 x 20 cm clear, polycarbonate cages in a windowless room. Horizontal mouse movement was recorded by 16 sensors (TSE-Systems, Inc., Chesterfield, MO) separated by 2.5 cm along the bottom of the locomotor box. Horizontal movement was detected and counted when there was a break in the infrared sensor. Activity counts were collected on a computer running Fusion HC software (AccuScan Instruments Inc., Columbus, OH).

Examining the efficiency of DAL-TRAM in reducing cocaine-induced hyperlocomotion and the specificity of the DAL-TRAM components

Drugs

DAL-TRAM and control variations were prepared as described under liposome preparation. Mice (n = 77) were assigned to the following conditions: DAL-TRAM/10 mg/mL cocaine (n = 8), DAL-TRAM/5 mg/mL cocaine (n = 8), DAL-TRAM/1 mg/mL cocaine (n = 7);

DAL-TRAM/saline (n = 8); TRAM/saline (n = 8); saline/saline (n = 6), Sub-TRAM/10 mg/mL cocaine (n =8); DAL/10 mg/mL cocaine (n=9); ROL-TRAM/10 mg/mL cocaine (n= 7); and TRAM/ 10 mg/mL cocaine (n= 8). Cocaine hydrochloride (Sigma-Aldrich, USA) was dissolved in 0.9% NaCl at a concentration of 10 mg/mL. The 10 mg/mL solution was also used to prepare the 5 mg/mL and 1 mg/mL doses. Cocaine was prepared within 24 hours of being used. To validate the system, mice (n= 40) were assigned to the following conditions in a separate experiment: Sub-TRAM + 10 mg/mL cocaine (n=7), DA20m-TRAM +10 mg/mL cocaine (n=8), DAL-TRAM + 10 mg/mL cocaine (n=8), DA20 m-TRAM + saline (n=9) and DAL-TRAM + saline (n=8). Cocaine was prepared as described above.

Behavioral Procedure

Mice were acclimated to the laboratory housing conditions for a minimum of 7 days prior to any experimental manipulations. Following this, all mice underwent a habituation phase to the locomotor apparatus that took place over 3 days. Mice remained in the locomotor cages for 30 min on each of 3 consecutive days. All habituation trials took place between 08:00 and 10:00 am. On the test day, DAL-TRAM or control variations (0.1 mL i.p.) were injected 5 min prior to cocaine or saline injection (0.1 mL i.p.). Five minutes after the cocaine injection, animals were placed in the locomotor apparatus and locomotor testing commenced. Locomotor activity was recorded in 5 min bins over a 30 min period.

Chronic administration of DAL-TRAM in saline treated animals

Drugs

DAL-TRAM and TRAM were prepared as described under liposome preparation. Mice were assigned to the following groups; DAL-TRAM (n= 5), TRAM (n= 5) or no injection (n= 5).

Behavioral Procedure

Mice were acclimated to the laboratory housing conditions for a minimum of 7 days prior to any experimental manipulations. Following this, all mice underwent a habituation phase to the locomotor apparatus that took place over 3 days. On each habituation day, mice were transported to the room containing the locomotor apparatus and individually placed into separate locomotor cages. Mice remained in the locomotor cages for 30 min on each of 3 consecutive days. All habituation trials took place between 08:00 and 10:00 am.

Depending on the group, mice received an i.p. injection (0.1 mL) of either DAL-TRAM or TRAM, or received no injection 5 min prior to placement in the locomotor apparatus on each of 6 test days following the habituation phase. On each test day, mice were placed in the locomotor apparatus and their horizontal activity was recorded in 5 min bins over a 30 min period.

Fluorescent histochemical Staining by Fluoro-Jade B

As an initial assessment of the toxicity of the DAL-TRAM and TRAM in a chronic model of administration mice were sacrificed by rapid decapitation. Brains were extracted and post fixed in a solution of 30% sucrose in 4% paraformaldehyde (PFA), were flash frozen, and then were cryostat sliced into 35 μm coronal sections. Frozen sections were mounted, were allowed to dry and then were washed 6 times for 10 minutes in 0.1M phosphate buffer (pH 7.4). Subsequently tissue was immersed in 100% ethanol (3 mins), 70% ethanol (2 mins), 30% ethanol (2 mins), and then distilled H_2O (2 mins). Sections were incubated in filtered 0.06% $KMnO_4$ for 15 minutes and then rinsed with distilled H_2O for 2 minutes. Next sections were incubated in 0.001% Fluoro-Jade B (EDM Millipore, Etobicoke, Canada) in 0.1% acetic acid solution for 30 minutes and then were briefly rinsed in distilled H_2O. Immediately following Fluoro-Jade B incubation sections were dried using a drier set on high for 2 minutes so that all excess water was

removed from the slides. Sections were then placed in Clearene Solvent (Leica Biosystems, Concord, Canada) for 2 minutes and were cover slipped using DPX Mountant for histology (Sigma-Aldrich Canada, Oakville, Canada).

Supporting Information: Additional materials and methods; S1: The secondary structure of DopaA20min as predicted by RNAstructure (A) and the nucleobase composition of the sequence (B); Table S1: Possible G-Quadruplexes predicted by QGRS Mapper; S2: Evaluation of DA20m secondary structure in the presence and absence of dopamine ; S3: Determination of the dissociation constant of DA20m using fluorescence anisotropy; S4: Synthesis of the multi-DNA aptamer payload targeting system; S5: Encapsulation of a control oligonucleotide into non-rhodamine labelled liposomes; S6: Characterization of homogeneity of the liposome targeting system by transmission electron microscopy (TEM); S7: Characterization of liposome stability in serum by TEM imaging; S8: Characterization of liposome stability over time by TEM and Nanoparticle Tracking Analysis; Table S2: Oligonucleotide sequences used in the multi-aptamer targeting/payload system design; S9: Fluorescence distribution of rhodamine labeled DAL-TRAM and DAL in nucleus accumbens tissue; Table S3: Analysis of complementary mouse genomic and transcript targets by NCBI Blast to the forward and reverse primer regions of the dopamine binding aptamer (DBA); S10: Estimation of DBA in prefrontal cortex tissue by optical density analysis; S11-S13: Administration of DAL-TRAM at A) 10 mg/mL (S11), B) 5 mg/mL (S12) and C) 1 mg/mL (S13) cocaine compared to dosage specific controls; S14: Cumulative horizontal locomotor activity of DA20m-TRAM compared to controls over an entire 30 min session.; S15: Chronic administration: locomotor activity by day.

Author contributions:

This collaborative effort was initiated by EMM, MCD and MRH. All aptamer selection and characterization, as well as all liposome synthesis and characterization experiments were conceptualized by EMM and MCD. Aptamer selection and characterization experiments were preformed by EMM. Liposome synthesis and characterization experiments were performed by

EMM with assistance from VH and AK. Animal experiments were conceptualized by MRH, KV, EMM, and MCD. Animal experiments were preformed and analysed by KV with assistance from MRH, ZD and EMM. The manuscript was prepared by EMM and edited by MCD and MRH.

Acknowledgements

We thank Marzena Sieczkos (Department of Neuroscience, Carleton University), Jianqun Wang (Nano Imaging Facility, Carleton University), Ray Eby (Particle Metrix), Joshua Callahan and Timothy Wilson (Department of Chemistry, Carleton University), and Jordan Dekrakker (Department of Neuroscience, Carleton University) for their contribution to this work. This work was supported by NSERC Individual Discovery Grants 315827 and 315779 awarded to Matthew R. Holahan and Maria C. DeRosa, respectively. The authors have no conflicts of interest to declare.

References

[1] McKeague M, McConnell EM, Cruz-Toledo J, Bernard ED, Pach A, Mastronardi E, et al. Analysis of In Vitro Aptamer Selection Parameters. J Mol Evol 2015;81:150–61. doi:10.1007/s00239-015-9708-6.

[2] Ellington AD, Szostak JW. In vitro selection of RNA molecules that bind specific ligands. Nature 1990;346:818–22. doi:10.1038/346818a0.

[3] Robertson DL, Joyce GF. Selection in vitro of an RNA enzyme that specifically cleaves single-stranded DNA. Nature 1990;344:467–8. doi:10.1038/344467a0.

[4] Tuerk C, Gold L. Systematic evolution of ligands by exponential enrichment: RNA ligands to bacteriophage T4 DNA polymerase. Science 1990;249:505–10. doi:10.1126/science.2200121.

[5] Ruigrok VJB, Levisson M, Eppink MHM, Smidt H, van der Oost J. Alternative affinity tools: more attractive than antibodies? Biochem J 2011;436:1–13. doi:10.1042/BJ20101860.

[6] Mayer G. The Chemical Biology of Aptamers. Angew Chemie Int Ed 2009;48:2672–89. doi:10.1002/anie.200804643.

[7] Keefe AD, Pai S, Ellington A. Aptamers as therapeutics. Nat Rev Drug Discov 2010;9:537–50. doi:10.1038/nrd3141.

[8] Bunka DHJ, Platonova O, Stockley PG. Development of aptamer therapeutics. Curr Opin Pharmacol 2010;10:557–62. doi:10.1016/j.coph.2010.06.009.

[9] Bouchard PR, Hutabarat RM, Thompson KM. Discovery and Development of Therapeutic Aptamers. Annu Rev Pharmacol Toxicol 2010;50:237–57. doi:10.1146/annurev.pharmtox.010909.105547.

[10] Famulok M, Mayer G. Intramers and Aptamers: Applications in Protein-Function Analyses and Potential for Drug Screening. ChemBioChem 2005;6:19–26. doi:10.1002/cbic.200400299.

[11] Soule EE, Bompiani KM, Woodruff RS, Sullenger BA. Targeting Two Coagulation Cascade Proteases with a Bivalent Aptamer Yields a Potent and Antidote-Controllable Anticoagulant. Nucleic Acid Ther 2015;26:1–9. doi:10.1089/nat.2015.0565.

[12] McConnell EM, Holahan MR, DeRosa MC. Aptamers as promising molecular recognition elements for diagnostics and therapeutics in the central nervous system. Nucleic Acid Ther 2014;24:388–404. doi:10.1089/nat.2014.0492.

[13] Röthlisberger P, Gasse C, Hollenstein M. Nucleic Acid Aptamers: Emerging Applications in Medical Imaging, Nanotechnology, Neurosciences, and Drug Delivery. Int J Mol Sci 2017;18:2430. doi:10.3390/ijms18112430.

[14] Bouvier-Müller A, Ducongé F. Nucleic acid aptamers for neurodegenerative diseases. Biochimie 2018;145:73–83. doi:10.1016/j.biochi.2017.10.026.

[15] Mannironi C, Di Nardo A, Fruscoloni P, Tocchini-Valentini GP. In vitro selection of dopamine RNA ligands. Biochemistry 1997;36:9726–34. doi:10.1021/bi9700633.

[16] Walsh R, DeRosa MC. Retention of function in the DNA homolog of the RNA dopamine aptamer. Biochem Biophys Res Commun 2009;388:732–5. doi:10.1016/j.bbrc.2009.08.084.

[17] Holahan MR, Madularu D, McConnell EM, Walsh R, DeRosa MC. Intra-accumbens injection of a dopamine aptamer abates MK-801-induced cognitive dysfunction in a model of schizophrenia. PLoS One 2011;6:e22239. doi:10.1371/journal.pone.0022239.

[18] Shi N, Boado RJ, Pardridge WM. Receptor-mediated Gene Targeting to Tissues In Vivo Following Intravenous Administration of Pegylated Immunoliposomes. Pharm Res 2001;18:1091–5. doi:10.1023/A:1010910523202.
[19] Shi N, Pardridge WM. Noninvasive gene targeting to the brain. Proc Natl Acad Sci U S A 2000;97:7567–72. doi:10.1073/pnas.130187497.
[20] Pardridge WM. Gene targeting in vivo with pegylated immunoliposomes. Methods Enzymol 2003;373:507–28. doi:10.1016/S0076-6879(03)73032-8.
[21] Pardridge WM. Molecular Trojan horses for blood-brain barrier drug delivery. Curr Opin Pharmacol 2006;6:494–500. doi:10.1016/j.coph.2006.06.001.
[22] Pardridge WM. Blood-brain barrier delivery of protein in non-viral gene therapeutics with molecular Trojan horses. J Control Release 2007;122:345–8. doi:10.1016/j.jconrel.2007.04.001.Blood-brain.
[23] Allen TM, Cullis PR. Liposomal drug delivery systems: From concept to clinical applications. Adv Drug Deliv Rev 2013;65:36–48. doi:10.1016/j.addr.2012.09.037.
[24] Nogueira E, Gomes AC, Preto A, Cavaco-Paulo A. Design of liposomal formulations for cell targeting. Colloids Surfaces B Biointerfaces 2015;136:514–26. doi:10.1016/j.colsurfb.2015.09.034.
[25] Simão AMS, Bolean M, Cury TAC, Stabeli RG, Itri R, Ciancaglini P. Liposomal systems as carriers for bioactive compounds. Biophys Rev 2015;7:391–7. doi:10.1007/s12551-015-0180-8.
[26] Shim MS, Kwon YJ. Efficient and targeted delivery of siRNA in vivo. FEBS J 2010;277:4814–27. doi:10.1111/j.1742-4658.2010.07904.x.
[27] Jiang F, Liu B, Lu J, Li F, Li D, Liang C, et al. Progress and Challenges in Developing Aptamer-Functionalized Targeted Drug Delivery Systems. Int J Mol Sci 2015;16:23784–822. doi:10.3390/ijms161023784.
[28] Cheng C, Chen YH, Lennox K a, Behlke M a, Davidson BL. In vivo SELEX for Identification of Brain-penetrating Aptamers. Mol Ther Nucleic Acids 2013;2:e67. doi:10.1038/mtna.2012.59.
[29] Deane R, Zheng W, Zlokovic B V. Brain capillary endothelium and choroid plexus epithelium regulate transport of transferrin-bound and free iron into the rat brain. J Neurochem 2004;88:813–20. doi:10.1046/j.1471-4159.2003.02221.x.
[30] de Lange ECM. The mastermind approach to CNS drug therapy: translational prediction of human brain distribution, target site kinetics, and therapeutic effects. Fluids Barriers CNS 2013;10:12–27. doi:10.1186/2045-8118-10-12.
[31] Dufès C, Al Robaian M, Somani S. Transferrin and the transferrin receptor for the targeted delivery of therapeutic agents to the brain and cancer cells. Ther Deliv 2013;4:629–40. doi:10.4155/tde.13.21.
[32] Clark AJ, Davis ME. Increased brain uptake of targeted nanoparticles by adding an acid-cleavable linkage between transferrin and the nanoparticle core. Proc Natl Acad Sci U S A 2015;112:12486–91. doi:10.1073/pnas.1517048112.
[33] Sehlin D, Fang XT, Cato L, Antoni G, Lannfelt L, Syvänen S. Antibody-based PET imaging of amyloid beta in mouse models of Alzheimer's disease. Nat Commun 2016;7:10759. doi:10.1038/ncomms10759.
[34] Cabezón I, Manich G, Martín-Venegas R, Camins A, Pelegrí C, Vilaplana J. Trafficking of Gold Nanoparticles Coated with the 8D3 Anti-Transferrin Receptor Antibody at the Mouse Blood-Brain Barrier. Mol Pharm 2015;12:4137–45.

doi:10.1021/acs.molpharmaceut.5b00597.
[35] Ko YT. Nanoparticle-mediated delivery of oligonucleotides to the blood–brain barrier: in vitro and in situ brain perfusion studies on the uptake mechanisms. J Drug Target 2013;21:866–73. doi:10.3109/1061186X.2013.829077.
[36] Chen CB, Dellamaggiore KR, Ouellette CP, Sedano CD, Lizadjohry M, Chernis G a, et al. Aptamer-based endocytosis of a lysosomal enzyme. Proc Natl Acad Sci U S A 2008;105:15908–13. doi:10.1073/pnas.0808360105.
[37] Porciani D, Signore G, Marchetti L, Mereghetti P, Nifosì R, Beltram F. Two interconvertible folds modulate the activity of a DNA aptamer against transferrin receptor. Mol Ther Nucleic Acids 2014;3:e144. doi:10.1038/mtna.2013.71.
[38] Macdonald J, Houghton P, Xiang D, Duan W, Shigdar S. Truncation and Mutation of a Transferrin Receptor Aptamer Enhances Binding Affinity. Nucleic Acid Ther 2016;26:348–54. doi:10.1089/nat.2015.0585.
[39] Zhang M-Z, Yu R-N, Chen J, Ma Z-Y, Zhao Y-D. Targeted quantum dots fluorescence probes functionalized with aptamer and peptide for transferrin receptor on tumor cells. Nanotechnology 2012;23:485104. doi:10.1088/0957-4484/23/48/485104.
[40] Hu J, Al-Waili D, Hassan A, Fan G-C, Xin M, Hao J. Inhibition of cerebral vascular inflammation by brain endothelium-targeted oligodeoxynucleotide complex. Neuroscience 2016;329:30–42. doi:10.1016/j.neuroscience.2016.04.033.
[41] Macdonald J, Henri J, Goodman L, Xiang D, Duan W, Shigdar S. Development of a Bifunctional Aptamer Targeting the Transferrin Receptor and Epithelial Cell Adhesion Molecule (EpCAM) for the Treatment of Brain Cancer Metastases. ACS Chem Neurosci 2017;8:777–84. doi:10.1021/acschemneuro.6b00369.
[42] Stoltenburg R, Reinemann C, Strehlitz B. FluMag-SELEX as an advantageous method for DNA aptamer selection. Anal Bioanal Chem 2005;383:83–91. doi:10.1007/s00216-005-3388-9.
[43] McKeague M, Derosa MC. Challenges and opportunities for small molecule aptamer development. J Nucleic Acids 2012;2012. doi:10.1155/2012/748913.
[44] McKeague M, McConnell EM, Cruz-Toledo J, Bernard ED, Pach A, Mastronardi E, et al. Analysis of In Vitro Aptamer Selection Parameters. J Mol Evol 2015;81. doi:10.1007/s00239-015-9708-6.
[45] Legiewicz M, Lozupone C, Knight R, Yarus M. Size, constant sequences, and optimal selection. RNA 2005;11:1701–9. doi:10.1261/rna.2161305.
[46] Mathews DH. RNA Secondary Structure Analysis Using RNAstructure. Curr Protoc Bioinformatics 2014;46:12.6.1-12.6.25. doi:10.1002/0471250953.bi1206s46.
[47] Luo X, McKeague M, Pitre S, Dumontier M, Green J, Golshani A, et al. Computational approaches toward the design of pools for the in vitro selection of complex aptamers. RNA 2010;16:2252–62. doi:10.1261/rna.2102210.
[48] Lee JF, Hesselberth JR, Meyers LA, Ellington AD. Aptamer Database. Nucleic Acids Res 2004;32:D95–100. doi:10.1093/nar/gkh094.
[49] Tucker WO, Tanner KTS and JA. G-quadruplex DNA Aptamers and their Ligands: Structure, Function and Application. Curr Pharm Des 2012;18:2014–26. doi:http://dx.doi.org/10.2174/138161212799958477.
[50] Gatto B, Palumbo M, Sissi C. Nucleic Acid Aptamers Based on the G-Quadruplex Structure: Therapeutic and Diagnostic Potential. Curr Med Chem 2009;16:1248–65. doi:10.2174/092986709787846640.

[51] Avino A, Fabrega C, Tintore M, Eritja R. Thrombin Binding Aptamer, More than a Simple Aptamer: Chemically Modified Derivatives and Biomedical Applications. Curr Pharm Des 2012;18:2036–47. doi:10.2174/138161212799958387.
[52] Kikin O, D'Antonio L, Bagga PS. QGRS Mapper: a web-based server for predicting G-quadruplexes in nucleotide sequences. Nucleic Acids Res 2006;34:W676-82. doi:10.1093/nar/gkl253.
[53] Tradigo G, Mannella L, Veltri P. Assessment of G-quadruplex prediction tools. Proc - IEEE Symp Comput Med Syst 2014:243–6. doi:10.1109/CBMS.2014.146.
[54] Park H, Paeng IR. Development of direct competitive enzyme-linked aptamer assay for determination of dopamine in serum. Anal Chim Acta 2011;685:65–73. doi:10.1016/j.aca.2010.11.010.
[55] Farjami E, Campos R, Nielsen JS, Gothelf K V, Kjems J, Ferapontova EE. RNA aptamer-based electrochemical biosensor for selective and label-free analysis of dopamine. Anal Chem 2013;85:121–8. doi:10.1021/ac302134s.
[56] Jiao L, Lu G, Zhang Q, Yuan Y, Wang J, Zhang C, et al. Aptamer and graphene-based electrochemical biosensor for dopamine determination with high sensitivity and selectivity. Micro Nano Lett 2013;8:903–5. doi:10.1049/mnl.2013.0626.
[57] Álvarez-Martos I, Campos R, Ferapontova EE. Surface state of the dopamine RNA aptamer affects specific recognition and binding of dopamine by the aptamer-modified electrodes. Analyst 2015;140:4089–96. doi:10.1039/c5an00480b.
[58] Álvarez-Martos I, Ferapontova EE. Electrochemical Label-Free Aptasensor for Specific Analysis of Dopamine in Serum in the Presence of Structurally Related Neurotransmitters. Anal Chem 2016;88:3608–16. doi:10.1021/acs.analchem.5b04207.
[59] Zheng Y, Wang Y, Yang X. Aptamer-based colorimetric biosensing of dopamine using unmodified gold nanoparticles. Sensors Actuators B Chem 2011;156:95–9. doi:10.1016/j.snb.2011.03.077.
[60] Liu S, Xing X, Yu J, Lian W, Li J, Cui M, et al. A novel label-free electrochemical aptasensor based on graphene-polyaniline composite film for dopamine determination. Biosens Bioelectron 2012;36:186–91. doi:10.1016/j.bios.2012.04.011.
[61] Li B-R, Hsieh Y-J, Chen Y-X, Chung Y-T, Pan C-Y, Chen Y-T. An ultrasensitive nanowire-transistor biosensor for detecting dopamine release from living PC12 cells under hypoxic stimulation. J Am Chem Soc 2013;135:16034–7. doi:10.1021/ja408485m.
[62] Zhou JW, Wang WY, Yu P, Xiong EH, Zhang XH, Chen JH. A simple label-free electrochemical aptasensor for dopamine detection. Rsc Adv 2014;4:52250–5. doi:10.1039/c4ra08090d.
[63] Hun X, Xu Y, Xie G, Luo X. Aptamer biosensor for highly sensitive and selective detection of dopamine using ubiquitous personal glucose meters. Sensors Actuators, B Chem 2015;209:596–601. doi:10.1016/j.snb.2014.11.135.
[64] Kim J, Rim YS, Chen H, Cao HH, Nakatsuka N, Al KIMET. Fabrication of High-Performance Ultrathin In 2 O 3 Film Field-E ff ect Transistors and Biosensors Using Chemical Lift-O ff Lithography. ACS Nano 2015;9:4572–82.
[65] Peters RF, Gutierrez-Rivera L, Dew SK, Stepanova M. Surface Enhanced Raman Spectroscopy Detection of Biomolecules Using EBL Fabricated Nanostructured Substrates. J Vis Exp 2015:1–17. doi:10.3791/52712.
[66] Walsh R, Ho U, Wang XL, DeRosa MC. Selective dopamine detection using aptamer-functionalized glassy carbon electrodes. Can J Chem 2015;93:572–7. doi:DOI

10.1139/cjc-2014-0444.
[67] Xu J, Li Y, Wang L, Huang Y, Liu D, Sun R, et al. A Facile Aptamer-based Sensing Strategy for Dopamine through the Fluorescence Resonance Energy Transfer between Rhodamine B and Gold Nanoparticles. Dye Pigment 2015;123:55–63. doi:10.1016/j.dyepig.2015.07.019.
[68] Zibaii MI, Latifi H, Asadollahi A, Bayat AH, Haghparast A. DNA aptamer-based fiber optic biosensor for selective and label-free detection of Dopamine. Proc SPIE 2015;9634:2–5. doi:10.1117/12.2193323.
[69] Gao L, Ju L, Cui H. Determination of the binding constant of specific interactions and binding target concentration simultaneously using a general chemiluminescence method. RSC Adv 2016;6:5305–11. doi:10.1039/C5RA24928G.
[70] Jarczewska M, Sheelam SR, Ziółkowski R, Górski Ł. A Label-Free Electrochemical DNA Aptasensor for the Detection of Dopamine. J Electrochem Soc 2016;163:B26–31. doi:10.1149/2.0501603jes.
[71] Liu L, Xia N, Meng J-J, Zhou B-B, Li S-J. An electrochemical aptasensor for sensitive and selective detection of dopamine based on signal amplification of electrochemical-chemical redox cycling. J Electroanal Chem 2016;775:58–63. doi:10.1016/j.jelechem.2016.05.028.
[72] Huang H, Shi S, Gao X, Gao R, Zhu Y, Wu X, et al. A universal label-free fluorescent aptasensor based on Ru complex and quantum dots for adenosine, dopamine and 17β-estradiol detection. Biosens Bioelectron 2016;79:198–204. doi:10.1016/j.bios.2015.12.024.
[73] Beiranvand S, Abbasi AR, Roushani M, Derikvand Z, Azadbakht A. A simple and label-free aptasensor based on amino group-functionalized gold nanocomposites-Prussian blue/carbon nanotubes as labels for signal amplification. J Electroanal Chem 2016;776:170–9. doi:10.1016/j.jelechem.2016.07.006.
[74] Azadbakht A, Roushani M, Abbasi AR, Menati S, Derikvand Z. A label-free aptasensor based on polyethyleneimine wrapped carbon nanotubes in situ formed gold nanoparticles as signal probe for highly sensitive detection of dopamine. Mater Sci Eng C 2016;68:585–93. doi:10.1016/j.msec.2016.05.077.
[75] Azadbakht A, Roushani M, Abbasi AR, Derikvand Z. Design and characterization of electrochemical dopamine–aptamer as convenient and integrated sensing platform. Anal Biochem 2016;507:47–57. doi:10.1016/j.ab.2016.04.022.
[76] Bahrami S, Abbasi AR, Roushani M, Derikvand Z, Azadbakht A. An electrochemical dopamine aptasensor incorporating silver nanoparticle, functionalized carbon nanotubes and graphene oxide for signal amplification. Talanta 2016;159:307–16. doi:10.1016/j.talanta.2016.05.060.
[77] Banerjee S, Hsieh Y-J, Liu C-R, Yeh N-H, Hung H-H, Lai Y-S, et al. Differential Releases of Dopamine and Neuropeptide Y from Histamine-Stimulated PC12 Cells Detected by an Aptamer-Modified Nanowire Transistor. Small 2016;12:5524–9. doi:10.1002/smll.201601370.
[78] Hwang Y, Park JY, Kwon OS, Joo S, Lee C-S, Bae J. Incorporation of hydrogel as a sensing medium for recycle of sensing material in chemical sensors. Appl Surf Sci 2018;429:258–63. doi:10.1016/j.apsusc.2017.06.243.
[79] Guo L, Hu Y, Zhang Z, Tang Y. Universal fluorometric aptasensor platform based on water-soluble conjugated polymers/graphene oxide. Anal Bioanal Chem 2018;410:287–

95. doi:10.1007/s00216-017-0720-0.
[80] Lin T, Wei K, Ju S, Huang C, Yang H. Diagnosis by simplicity: an aptachip for dopamine capture and accurate detection with a dual colorimetric and fluorometric system. J Mater Chem B 2018;6:3387–94. doi:10.1039/C8TB00913A.
[81] Talemi RP, Mousavi SM, Afruzi H. Using gold nanostars modified pencil graphite electrode as a novel substrate for design a sensitive and selective Dopamine aptasensor. Mater Sci Eng C 2017;73:700–8. doi:10.1016/j.msec.2016.12.119.
[82] Jin H, Zhao C, Gui R, Gao X, Wang Z. Reduced graphene oxide/nile blue/gold nanoparticles complex-modified glassy carbon electrode used as a sensitive and label-free aptasensor for ratiometric electrochemical sensing of dopamine. Anal Chim Acta 2018;1025:154–62. doi:10.1016/j.aca.2018.03.036.
[83] Zibaii MI, Latifi H, Asadollahi A, Bayat AH, Dargahi L, Haghparast A. Label Free Fiber Optic Apta-Biosensor for <italic>In-Vitro</italic> Detection of Dopamine. J Light Technol 2016;34:4516–24. doi:10.1109/JLT.2016.2550533.
[84] Zhu L, Xu G, Song Q, Tang T, Wang X, Wei F, et al. Highly sensitive determination of dopamine by a turn-on fluorescent biosensor based on aptamer labeled carbon dots and nano-graphite. Sensors Actuators B Chem 2016;231:506–12. doi:10.1016/j.snb.2016.03.084.
[85] Zhang Y, Qi S, Liu Z, Shi Y, Yue W, Yi C. Rapid determination of dopamine in human plasma using a gold nanoparticle-based dual-mode sensing system. Mater Sci Eng C Mater Biol Appl 2016;61:207–13. doi:10.1016/j.msec.2015.12.038.
[86] Chen T, Tang L, Yang F, Zhao Q, Jin X, Ning Y, et al. Electrochemical Determination of Dopamine by a Reduced Graphene Oxide–Gold Nanoparticle-Modified Glassy Carbon Electrode. Anal Lett 2016;49:2223–33. doi:10.1080/00032719.2016.1142558.
[87] Kim E, Paeng IR. Advantageous sensitivity in the DNA homolog of the RNA dopamine aptamer. J Immunoassay Immunochem 2014;35:83–100. doi:10.1080/15321819.2013.792833.
[88] Perschbacher K, Smestad J a, Peters JP, Standiford MM, Denic A, Wootla B, et al. Quantitative PCR analysis of DNA aptamer pharmacokinetics in mice. Nucleic Acid Ther 2015;25:11–9. doi:10.1089/nat.2014.0515.
[89] Merino M, Zalba S, Garrido MJ. Immunoliposomes in clinical oncology: State of the art and future perspectives. J Control Release 2018;275:162–76. doi:10.1016/j.jconrel.2018.02.015.
[90] Chen C, Yang Z, Tang X. Chemical modifications of nucleic acid drugs and their delivery systems for gene-based therapy. Med Res Rev 2018;38:829–69. doi:10.1002/med.21479.
[91] Rivest V, Phivilay A, Julien C, Bélanger S, Tremblay C, Émond V, et al. Novel liposomal formulation for targeted gene delivery. Pharm Res 2007;24:981–90. doi:10.1007/s11095-006-9224-x.
[92] Bruno JG. Predicting the uncertain future of aptamer-based diagnostics and therapeutics. Molecules 2015;20:6866–87. doi:10.3390/molecules20046866.
[93] Skjørringe T, Gjetting T, Jensen TG. A modified protocol for efficient DNA encapsulation into pegylated immunoliposomes (PILs). J Control Release 2009;139:140–5. doi:10.1016/j.jconrel.2009.06.009.
[94] Chen C, Zhu S, Huang T, Wang S, Yan X. Analytical techniques for single-liposome characterization. Anal Methods 2013;5:2150. doi:10.1039/c3ay40219c.
[95] Altschul SF, Madden TL, Schäffer AA, Zhang J, Zhang Z, Miller W, et al. Gapped

BLAST and PSI-BLAST: a new generation of protein database search programs. Nucleic Acids Res 1997;25:3389–402.
[96] Ye J, Coulouris G, Zaretskaya I, Cutcutache I, Rozen S, Madden TL. Primer-BLAST: A tool to design target-specific primers for polymerase chain reaction. BMC Bioinformatics 2012;13:134. doi:10.1186/1471-2105-13-134.
[97] Beninger RJ, Banasikowski TJ. Dopaminergic mechanism of reward-related incentive learning: focus on the dopamine D(3) receptor. Neurotox Res 2008;14:57–70. doi:10.1007/BF03033575.
[98] Levy D, Shabat-Simon M, Shalev U, Barnea-Ygael N, Cooper A, Zangen A. Repeated Electrical Stimulation of Reward-Related Brain Regions Affects Cocaine But Not "Natural" Reinforcement. J Neurosci 2007;27:14179–89. doi:10.1523/JNEUROSCI.4477-07.2007.
[99] Werner F-M, Coveñas R. Safety of antipsychotic drugs: focus on therapeutic and adverse effects. Expert Opin Drug Saf 2014;13:1031–42. doi:10.1517/14740338.2014.935761.
[100] Schmued LC, Hopkins KJ. Fluoro-Jade B: a high affinity fluorescent marker for the localization of neuronal degeneration. Brain Res 2000;874:123–30. doi:10.1016/S0006-8993(00)02513-0.
[101] Wartman BC, Gabel J, Holahan MR. Inactivation of the Anterior Cingulate Reveals Enhanced Reliance on Cortical Networks for Remote Spatial Memory Retrieval after Sequential Memory Processing. PLoS One 2014;9:e108711. doi:10.1371/journal.pone.0108711.
[102] Kuroda KO, Ornthanalai VG, Kato T, Murphy NP. FosB Null Mutant Mice Show Enhanced Methamphetamine Neurotoxicity: Potential Involvement of FosB in Intracellular Feedback Signaling and Astroglial Function. Neuropsychopharmacology 2010;35:641–55. doi:10.1038/npp.2009.169.
[103] Schluesener HJ, Seid K, Deininger M, Schwab J. Transient in vivo activation of rat brain macrophages/microglial cells and astrocytes by immunostimulatory multiple CpG oligonucleotides. J Neuroimmunol 2001;113:89–94. doi:10.1016/S0165-5728(00)00428-8.
[104] Rohloff JC, Gelinas AD, Jarvis TC, Ochsner UA, Schneider DJ, Gold L, et al. Nucleic Acid Ligands With Protein-like Side Chains: Modified Aptamers and Their Use as Diagnostic and Therapeutic Agents. Mol Ther Nucleic Acids 2014;3:e201. doi:10.1038/mtna.2014.49.
[105] Famulok M, Hartig JS, Mayer G. Functional Aptamers and Aptazymes in Biotechnology, Diagnostics, and Therapy. Chem Rev 2007;107:3715–43. doi:10.1021/cr0306743.
[106] Luedtke NW, Tor Y. Fluorescence-based methods for evaluating the RNA affinity and specificity of HIV-1 Rev-RRE inhibitors. Biopolymers 2003;70:103–19. doi:10.1002/bip.10428.
[107] McConnell EM, Bolzon R, Mezin P, Frahm G, Johnston M, DeRosa MC. pHAST (pH-Driven Aptamer Switch for Thrombin) Catch-and-Release of Target Protein. Bioconjug Chem 2016;27:1493–9. doi:10.1021/acs.bioconjchem.6b00124.
[108] Montanari, JAM, Bucci, PL, Alonso, SdV. A Model Based in the Radius of Vesicles to Predict the Number of Unilamellar Liposomes. IJRPC 2014;4:484-9.
[109] Hermanson GT. Tags and Probes. Bioconjugate Tech., Elsevier; 1996, p. 297–416. doi:10.1016/B978-012342335-1/50009-9.

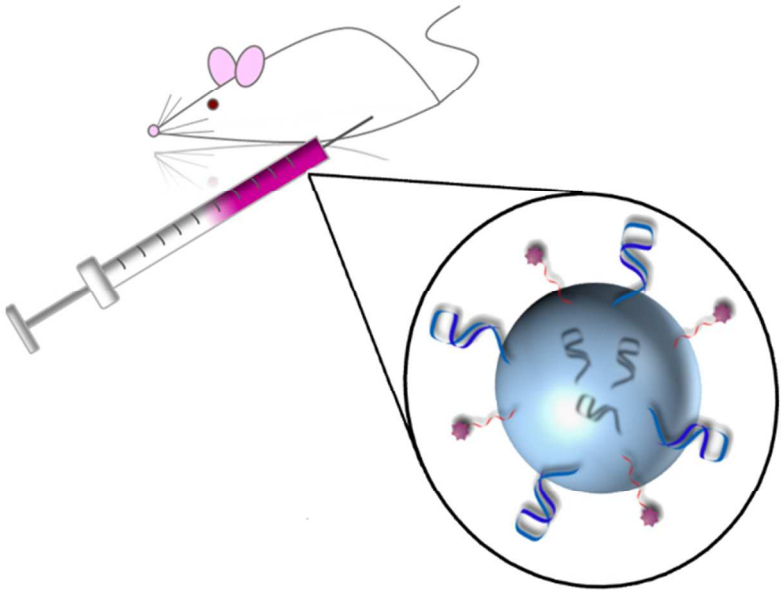

216x130mm (96 x 96 DPI)